Bio–Inspired Reduction and Robustness of Dynamic Robot Gaits

Sam Burden

Department of Electrical Engineering and Computer Sciences
University of California, Berkeley, CA, USA

October 24, 2013

Animals are extremely adept at dynamic locomotion

flat–terrain gait

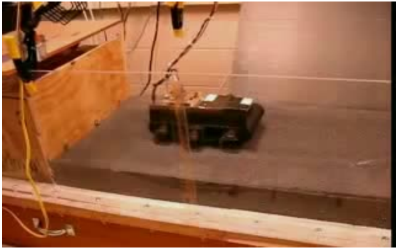

optimized gait

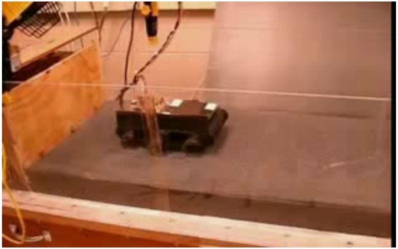

Sandbot RHex robot; Li *et al.* PNAS 2009

zebra–tailed lizard; Li *et al.* JEB 2012

Animal gaits exhibit surprising phenomena

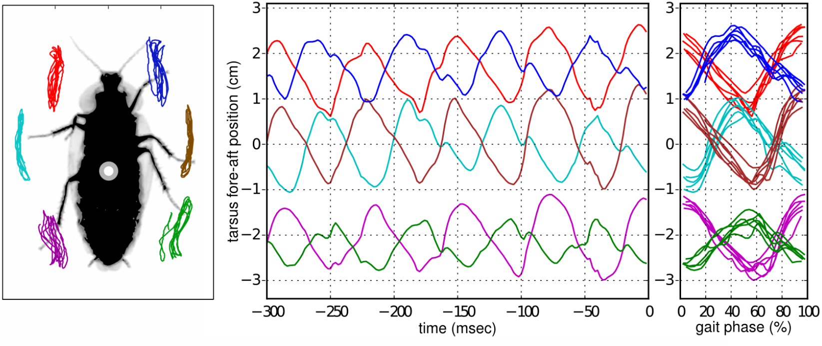

Animal gaits exhibit surprising phenomena

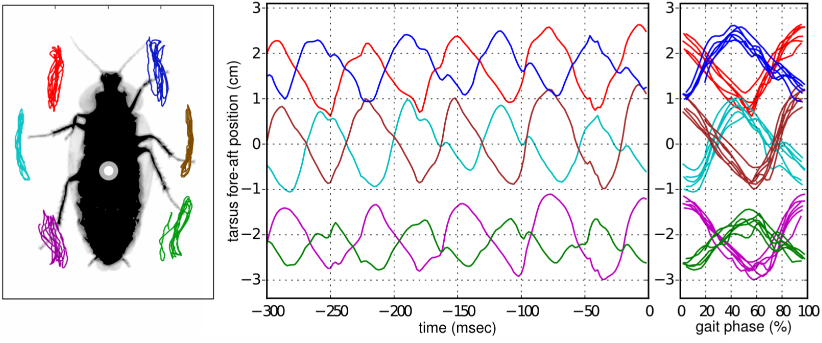

Reduction in degrees–of–freedom (DOF)

Cockroach dynamics ~ 7 dimensional (Revzen & Guckenheimer JRSI 2011)

Animal gaits exhibit surprising phenomena

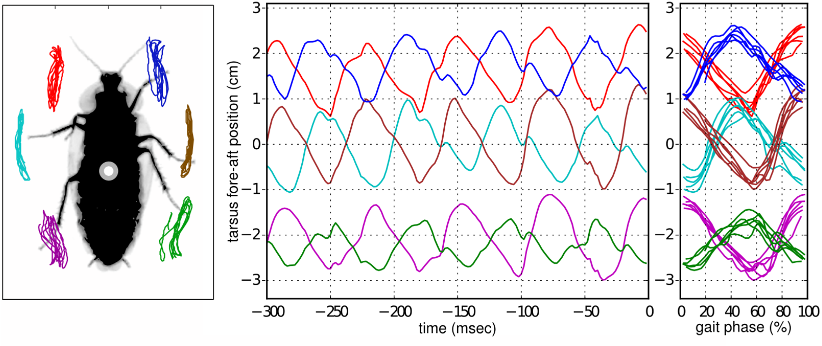

Reduction in degrees–of–freedom (DOF)

Cockroach dynamics ~ 7 dimensional (Revzen & Guckenheimer JRSI 2011)

Near–simultaneous limb touchdown

Quadrupeds *trot*, hexapods *alternate tripods* (Golubitsky *et al.* Nature 1999)

Empirically, animals use few degrees-of-freedom

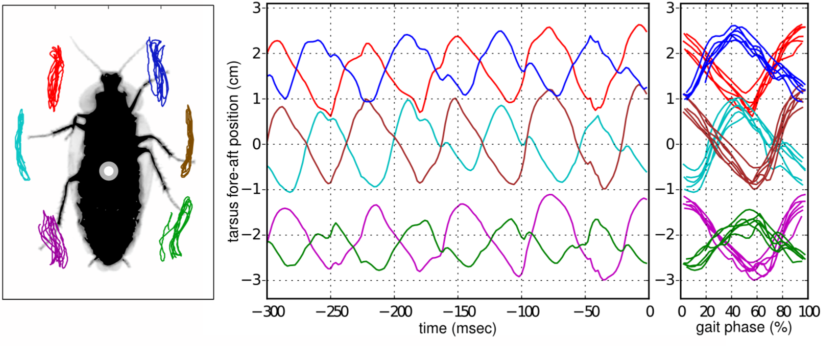

Empirically, animals use few degrees-of-freedom

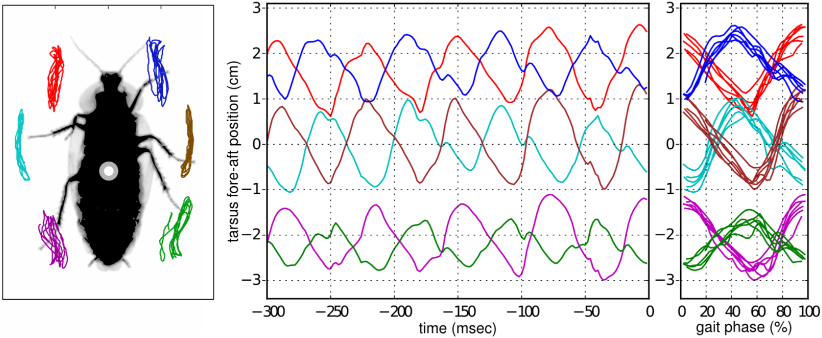

Mechanisms for reduction in neural or environmental models

Neural synchronization

Cohen et al. J. Math. Bio 1982

Physiological symmetry

Golubitsky et al. Nature 1999

Muscle activation synergy

Ting & Macpherson J. Neurosci. 2005

Granular media solidification

Li et al. Science 2013

Empirically, animals use few degrees-of-freedom

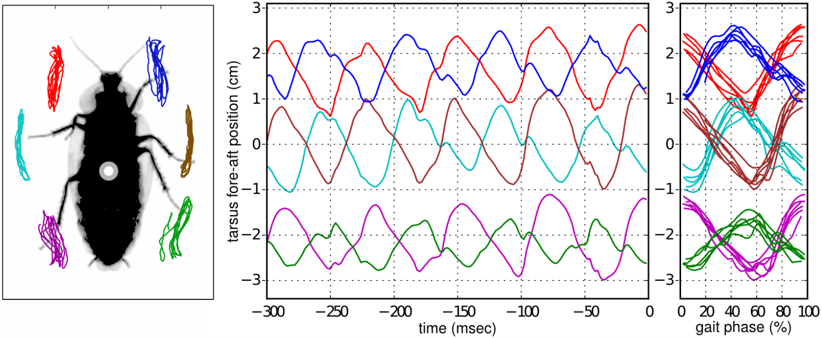

Mechanisms for reduction in neural or environmental models

Neural synchronization

Cohen et al. J. Math. Bio 1982

Physiological symmetry

Golubitsky et al. Nature 1999

Muscle activation synergy

Ting & Macpherson J. Neurosci. 2005

Granular media solidification

Li et al. Science 2013

Need model reduction tools for piecewise–defined (*hybrid*) dynamics

Use reduced–order models to study animal and robot gaits

physical system

animal, robot

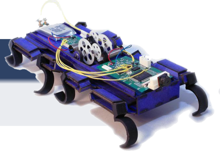

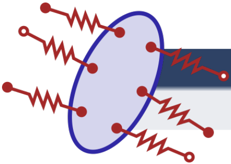

detailed model

10–100 DOF

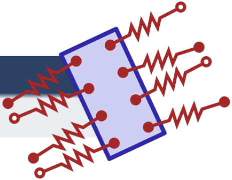

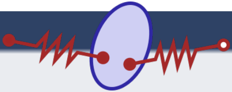

reduced-order model

< 10 DOF

Use reduced–order models to study animal and robot gaits

physical system

animal, robot

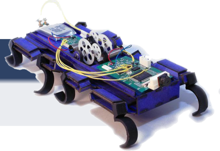

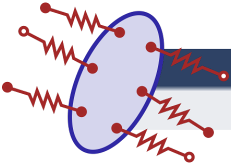

detailed model

10–100 DOF

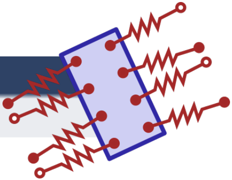

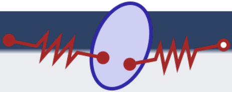

reduced-order model

< 10 DOF

Full & Koditschek JEB 1999

Use reduced–order models to study animal and robot gaits

physical system

animal, robot

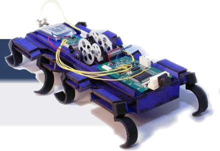

?

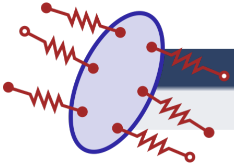

detailed model

10–100 DOF

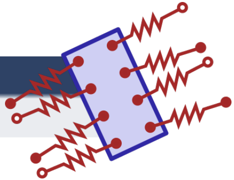

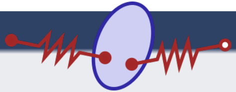

reduced-order model

< 10 DOF

Use reduced–order models to study animal and robot gaits

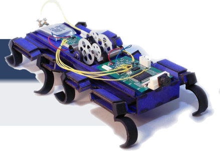

physical system

animal, robot

?

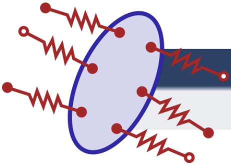

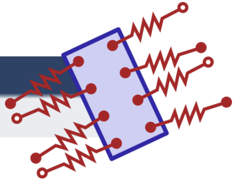

detailed model

10–100 DOF

?

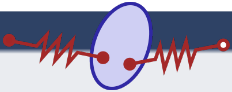

reduced-order model

< 10 DOF

Use reduced–order models to study animal and robot gaits

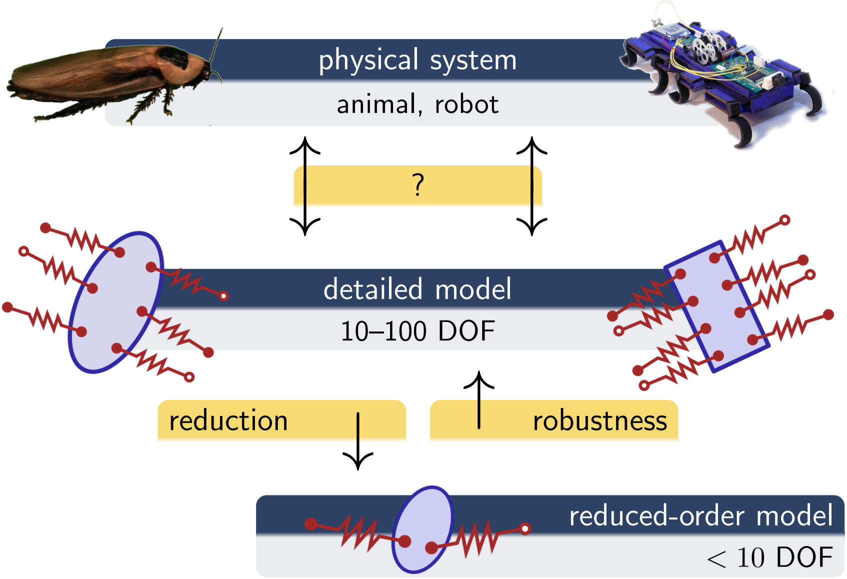

Use reduced–order models to study animal and robot gaits

physical system

animal, robot

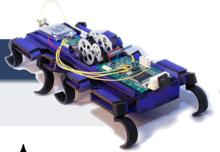

identification ↓

synthesis ↑

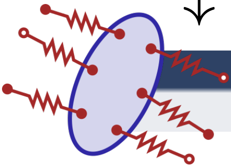

detailed model

10–100 DOF

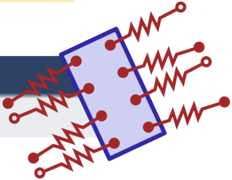

reduction ↓

robustness ↑

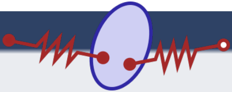

reduced-order model

< 10 DOF

Overview

Reduction

hybrid dynamics reduce dimensionality near periodic orbits

Identification

reduction enables scalable algorithm for parameter estimation

Robustness

near–simultaneous impacts lend robust stability to gaits

Synthesis

robustness enables synthesis of gaits and optimal maneuvers

Model Reduction

physical system

animal, robot

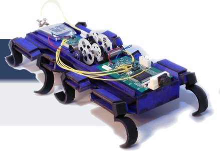

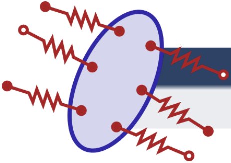

detailed model

10–100 DOF

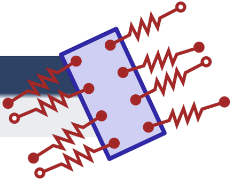

reduction $\downarrow$

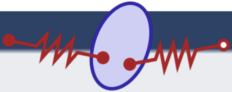

reduced-order model

< 10 DOF

Dimension loss in vertical hopper

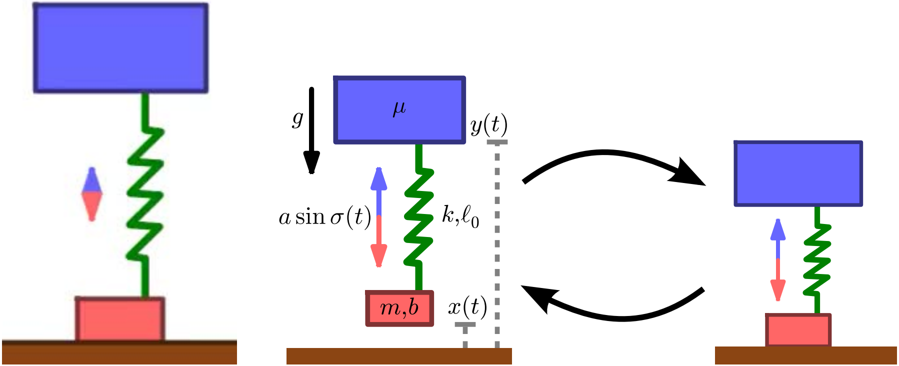

Dimension loss in vertical hopper

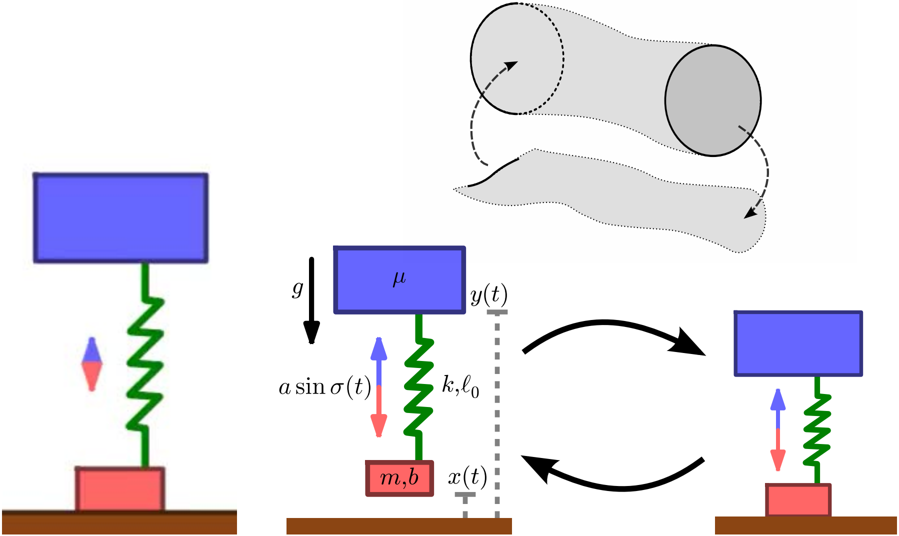

Hybrid dynamical system

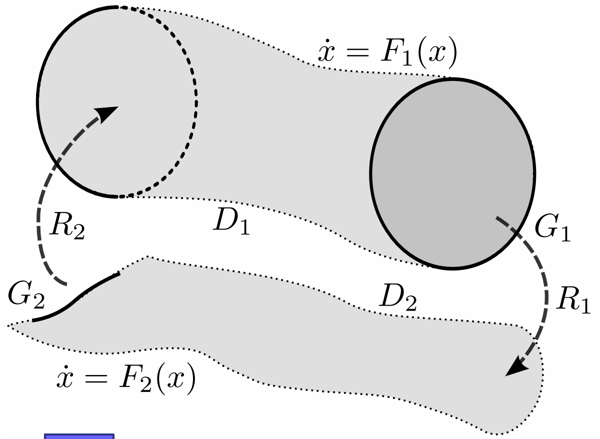

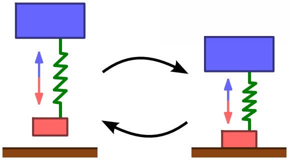

Trajectory for a hybrid dynamical system

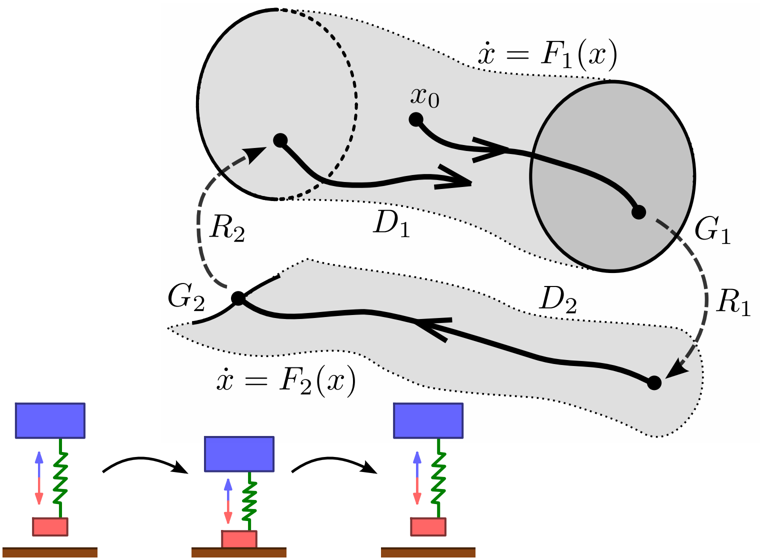

Trajectory for a hybrid dynamical system

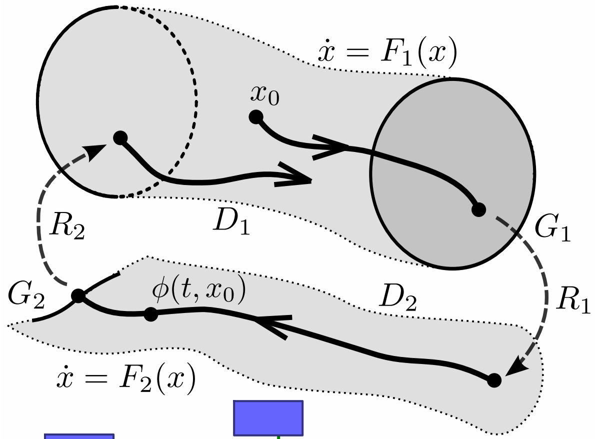

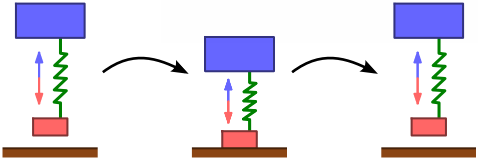

Periodic orbit γ for a hybrid dynamical system

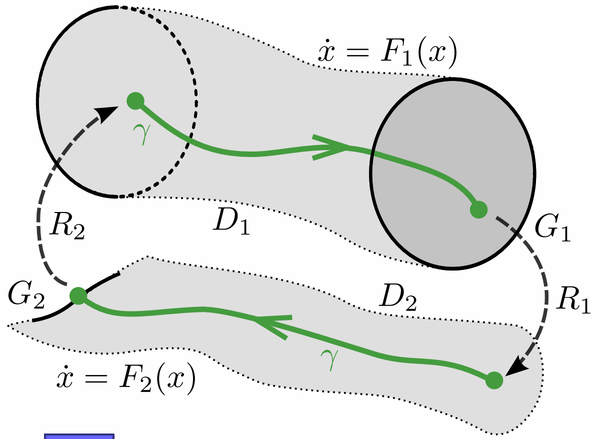

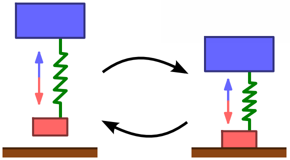

Assumptions on hybrid periodic orbit γ

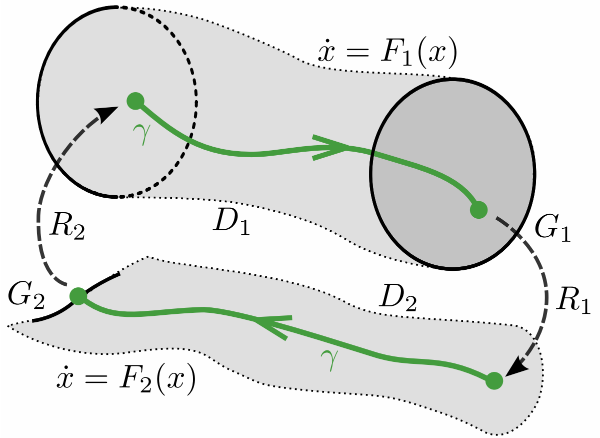

Assumption (transversality)

periodic orbit γ passes transversely through each guard G_j

Assumptions on hybrid periodic orbit γ

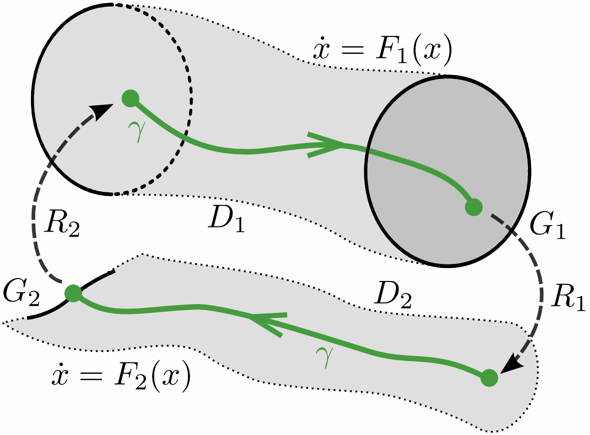

Assumption (isolated transitions)

$\exists \varepsilon > 0$: *periodic orbit* γ *spends at least* ε *time units in each domain* D_j

Poincaré map for periodic orbit γ

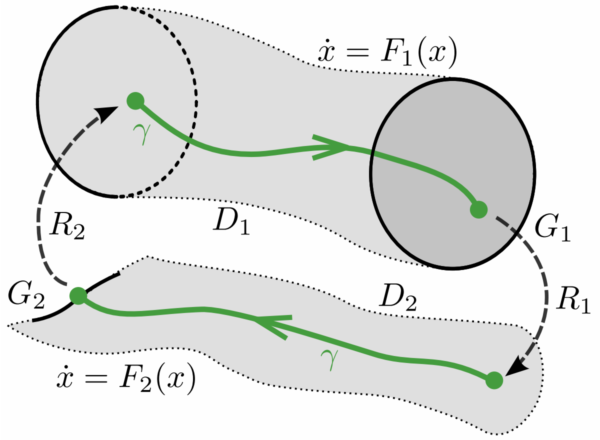

Poincaré map for periodic orbit γ

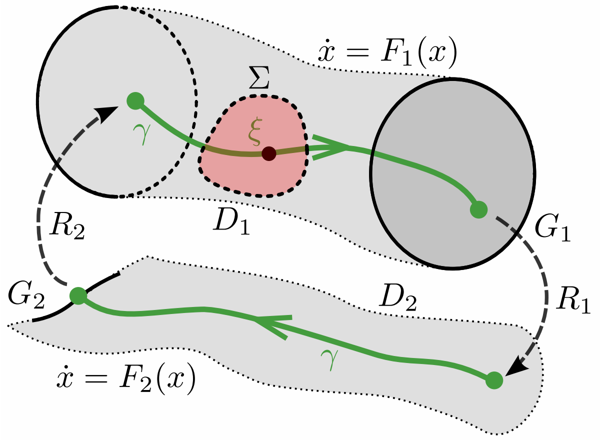

Poincaré map for periodic orbit γ

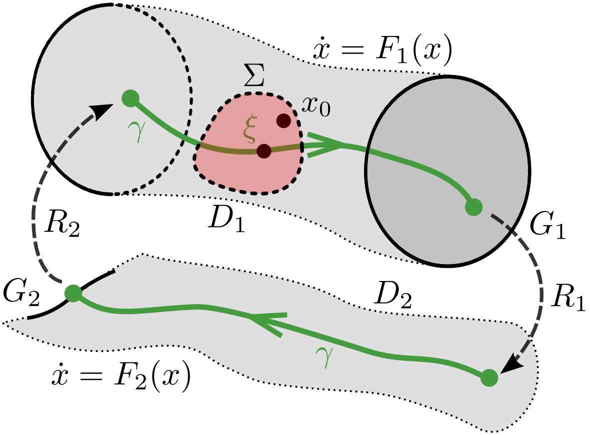

Poincaré map for periodic orbit γ

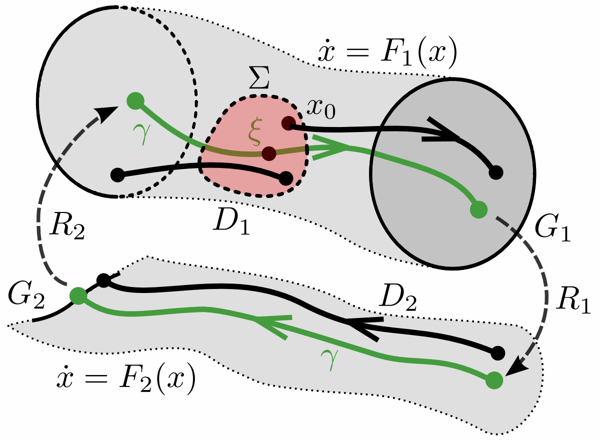

Poincaré map for periodic orbit γ

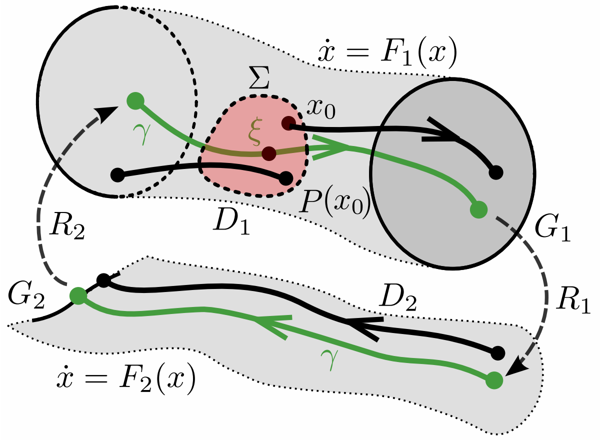

Poincaré map for periodic orbit γ

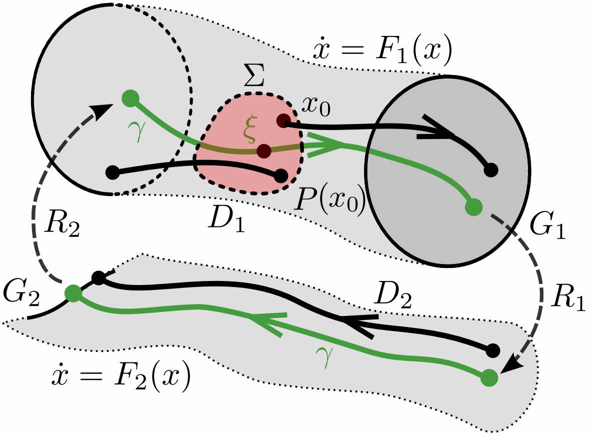

Theorem (Grizzle et al. TAC 2002)

The Poincaré map P is smooth in a neighborhood of ξ.

Model reduction near hybrid periodic orbit γ

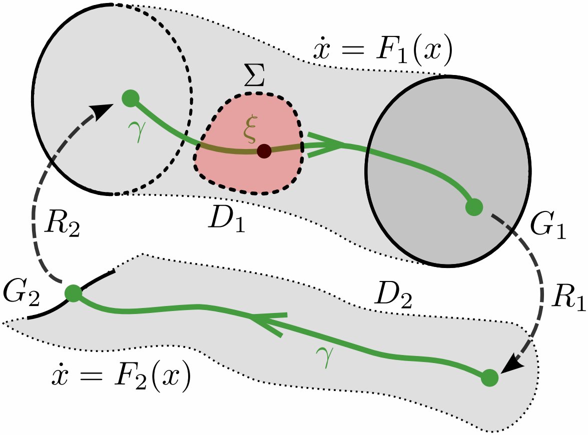

Model reduction near hybrid periodic orbit γ

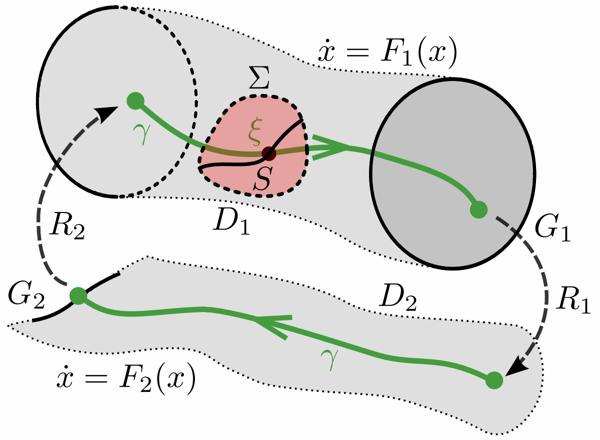

Model reduction near hybrid periodic orbit γ

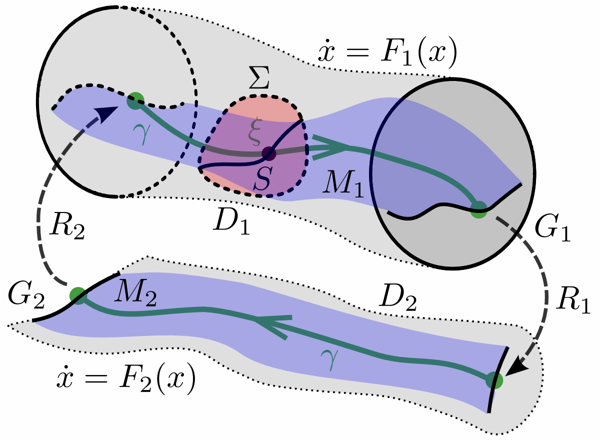

Model reduction near hybrid periodic orbit γ

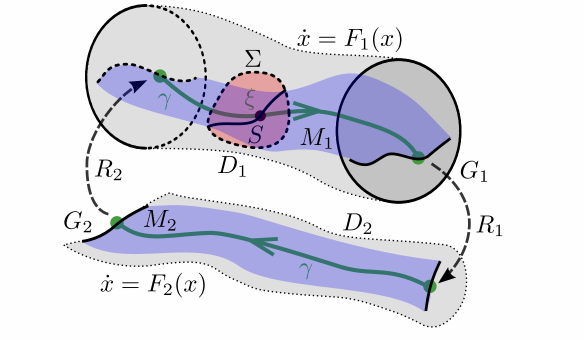

Theorem (Burden, Revzen, Sastry 2013 (arXiv:1308.4158))

Let $n = \min_j \dim D_j - 1$*. If* $\operatorname{rank} DP^n = r$ *near* ξ*, then trajectories starting near* γ *contract to a collection of hybrid-invariant* $(r+1)$*–dimensional submanifolds* $M_j \subset D_j$ *in finite time.*

Model reduction near hybrid periodic orbit γ

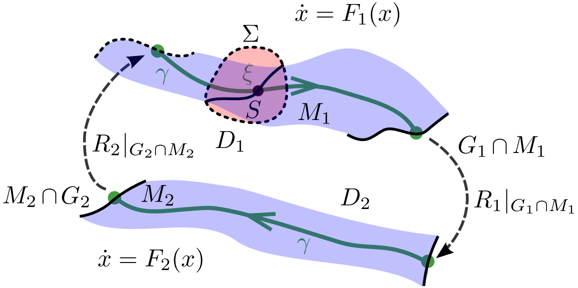

Corollary (Burden, Revzen, Sastry 2013 (arXiv:1308.4158))

The submanifolds M_j determine a hybrid system with periodic orbit γ.

Model reduction near hybrid periodic orbit γ

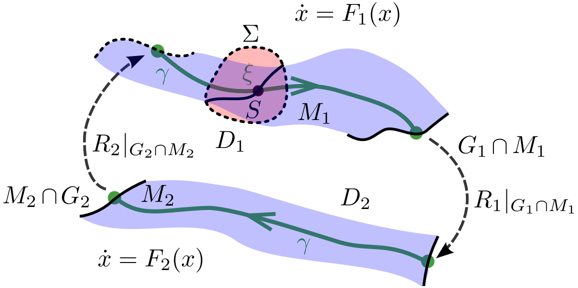

Corollary (Burden, Revzen, Sastry 2013 (arXiv:1308.4158))

The submanifolds M_j determine a hybrid system with periodic orbit γ.

γ is asymptotically stable in the original hybrid system

$\iff$ γ is asymptotically stable in the reduced hybrid system.

Spontaneous reduction in vertical hopper

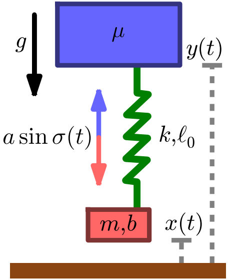

Numerically linearizing Poincaré map P on ground,
we find $DP(\xi)$ has eigenvalue $\simeq 0.57$,
therefore DP^2 is constant rank near ξ.

Spontaneous reduction in vertical hopper

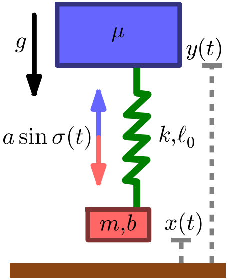

Numerically linearizing Poincaré map P on ground,
we find $DP(\xi)$ has eigenvalue $\simeq 0.57$,
therefore DP^2 is constant rank near ξ.

Corollary (Burden, Revzen, Sastry 2013 (arXiv:1308.4158))

2–DOF hopper contracts to 1–DOF hopper after one "hop".

Spontaneous reduction in vertical hopper

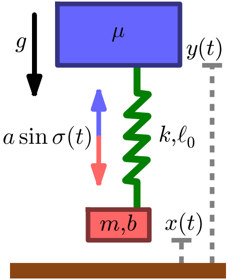

Numerically linearizing Poincaré map P on ground,
we find $DP(\xi)$ has eigenvalue $\simeq 0.57$,
therefore DP^2 is constant rank near ξ.

Corollary (Burden, Revzen, Sastry 2013 (arXiv:1308.4158))

2–DOF hopper contracts to 1–DOF hopper after one "hop".

Interpretation

Holonomic ground contact constraint persists after liftoff.

n–leg polyped reduces to Lateral Leg–Spring

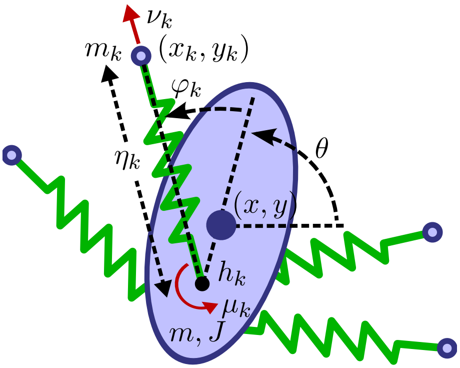

$(3 + 2n)$ DOF polyped

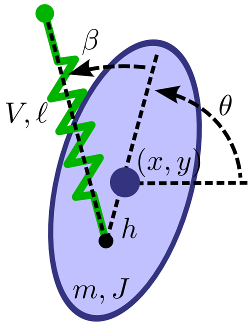

3 DOF Lateral Leg–Spring (LLS)

n–leg polyped reduces to Lateral Leg–Spring

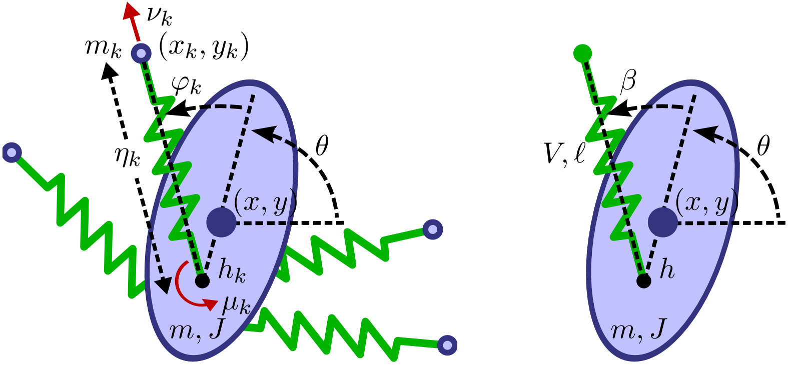

$(3 + 2n)$ DOF polyped

3 DOF Lateral Leg–Spring (LLS)

Controller (Burden, Revzen, Sastry 2013 (arXiv:1308.4158))

Smooth state feedback law reduces polyped to LLS after one stride.

Parameter Identification

physical system

animal, robot

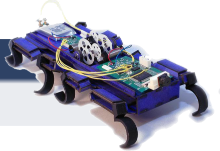

identification

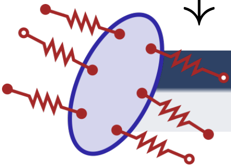

detailed model

10–100 DOF

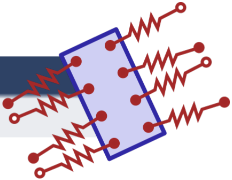

reduction

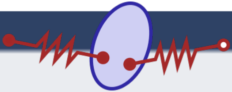

reduced-order model

< 10 DOF

Identification of initial conditions

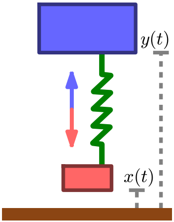

Identification of initial conditions

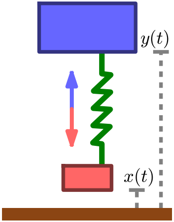

$$Y(\phi(t,z)) = y(t)$$

Identification of initial conditions

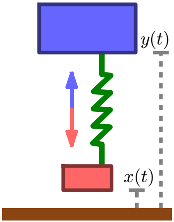

$$Y(\phi(t,z)) = y(t)$$

$$\eta_i = Y(\phi(iT, z^*)) + w_i,$$

w_i iid random variables

Identification of initial conditions

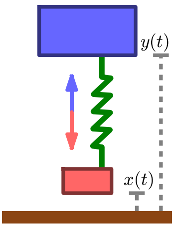

$$Y(\phi(t,z)) = y(t) \qquad \eta_i = Y(\phi(iT, z^*)) + w_i,$$

w_i iid random variables

Identification problem

Solve $\arg\min_{z \in D_j} \varepsilon\left(z, \{\eta_i\}\right)$, where $\varepsilon\left(z, \{\eta_i\}\right) := \sum_i \|Y(\phi(iT, z)) - \eta_i\|^2$.

Identification of initial conditions

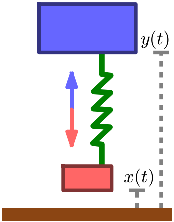

$Y(\phi(t,z)) = y(t)$ $\eta_i = Y(\phi(iT, z^*)) + w_i$,
w_i iid random variables

Identification problem

Solve $\arg\min_{z \in D_j} \varepsilon(z, \{\eta_i\})$, where $\varepsilon(z, \{\eta_i\}) := \sum_i \|Y(\phi(iT, z)) - \eta_i\|^2$.

Assumption (smooth observations)

Y is smooth along trajectories, i.e. $Y(\phi(t,z))$ is a smooth function of t.

Identification on original hybrid model vs. reduced model

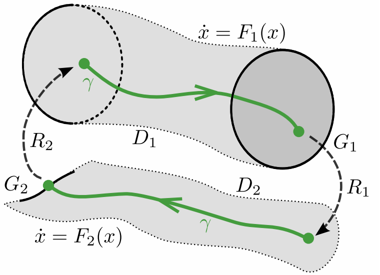

Identification on $\bigcup_j D_j$

$$\arg\min_{z \in D_j} \varepsilon\left(z, \{\eta_i\}\right)$$

Identification on original hybrid model vs. reduced model

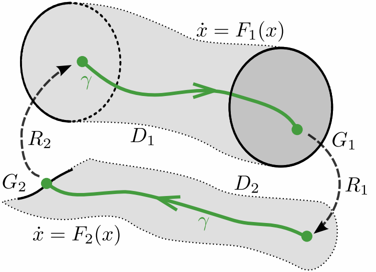

Identification on $\bigcup_j D_j$

$$\arg\min_{z \in D_j} \varepsilon\left(z, \{\eta_i\}\right)$$

$\nabla\varepsilon$ undefined on $G_j \subset D_j$

R_j not generally invertible

Identification on original hybrid model vs. reduced model

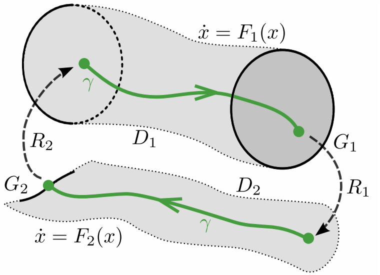

Identification on $\bigcup_j D_j$

$$\arg\min_{z \in D_j} \varepsilon\left(z, \{\eta_i\}\right)$$

$\nabla\varepsilon$ undefined on $G_j \subset D_j$

R_j not generally invertible

global optimization needed

Identification on original hybrid model vs. reduced model

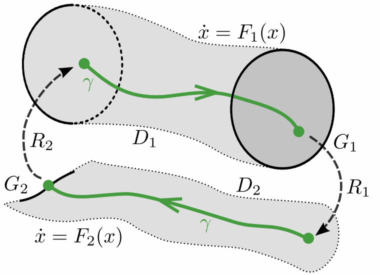

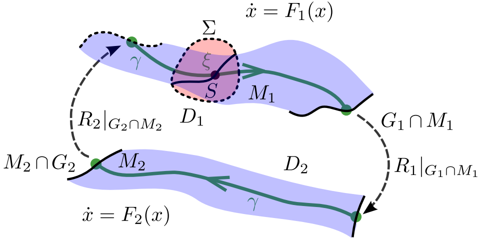

Identification on $\bigcup_j D_j$

$$\arg\min_{z \in D_j} \varepsilon\left(z, \{\eta_i\}\right)$$

Identification on $\bigcup_j M_j$

$$\arg\min_{z \in M_j} \varepsilon\left(z, \{\eta_i\}\right)$$

$\nabla\varepsilon$ undefined on $G_j \subset D_j$

R_j not generally invertible

global optimization needed

Burden, Ohlsson, Sastry SysID 2012

Identification on original hybrid model vs. reduced model

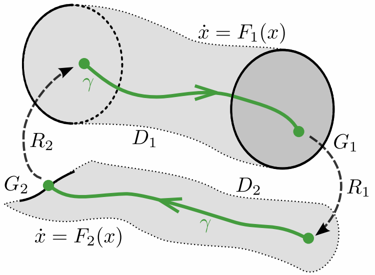

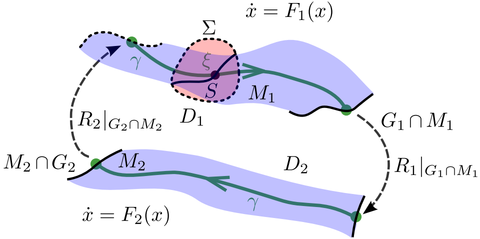

Identification on $\bigcup_j D_j$

$$\arg\min_{z \in D_j} \varepsilon\left(z, \{\eta_i\}\right)$$

Identification on $\bigcup_j M_j$

$$\arg\min_{z \in M_j} \varepsilon\left(z, \{\eta_i\}\right)$$

$\nabla\varepsilon$ undefined on $G_j \subset D_j$

R_j not generally invertible

global optimization needed

$\nabla\varepsilon$ well-defined on $G_j \cap M_j$

$R_j|_{M_j}$ invertible

Burden, Ohlsson, Sastry SysID 2012

Identification on original hybrid model vs. reduced model

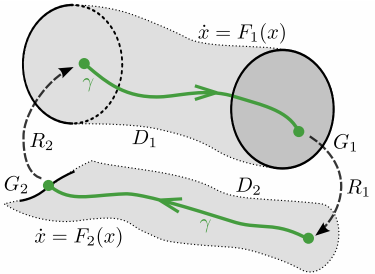

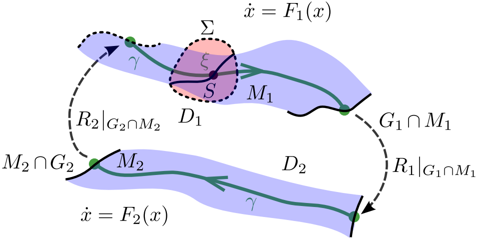

Identification on $\bigcup_j D_j$

$$\arg\min_{z \in D_j} \varepsilon\left(z, \{\eta_i\}\right)$$

$\nabla\varepsilon$ undefined on $G_j \subset D_j$

R_j not generally invertible

global optimization needed

Identification on $\bigcup_j M_j$

$$\arg\min_{z \in M_j} \varepsilon\left(z, \{\eta_i\}\right)$$

$\nabla\varepsilon$ well-defined on $G_j \cap M_j$

$R_j|_{M_j}$ invertible

first–order algorithms applicable

Burden, Ohlsson, Sastry SysID 2012

Novel quantitative predictions for biomechanics

observation

neural feedback appears at a delay

Revzen, Burden et al. BC 2013

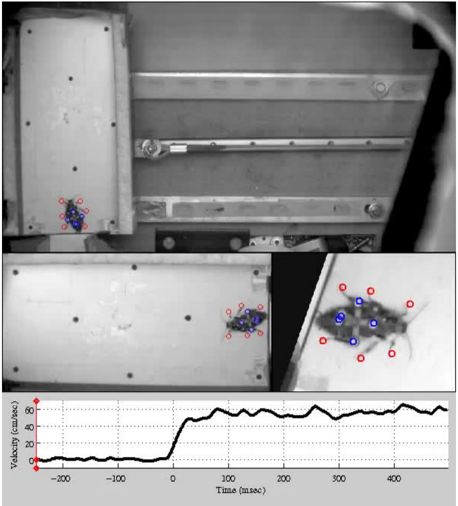

Novel quantitative predictions for biomechanics

observation

neural feedback appears at a delay

Revzen, Burden et al. BC 2013

identification

prediction

passive mechanics sensitive to inertia

Full et al. 2002

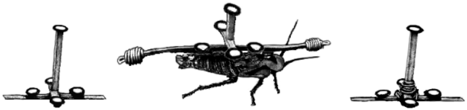

Burden, Revzen, Moore, Sastry, Full SICB 2013

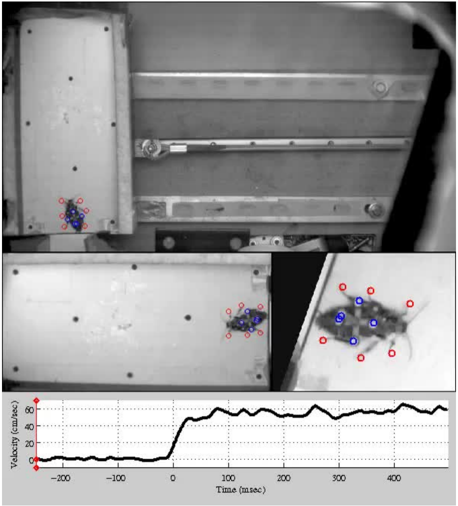

Model-based design and control of dynamic robots

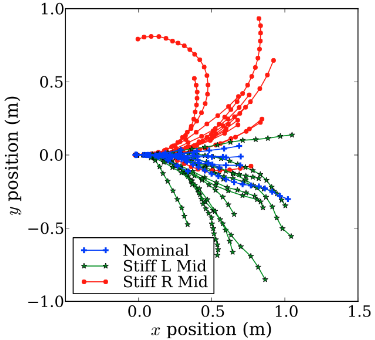

design

minimal use of actuators

Hoover et al. 2010

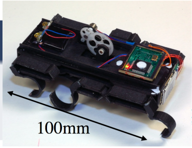

Hoover, Burden, Fu, Sastry, Fearing BIOROB 2010

Model-based design and control of dynamic robots

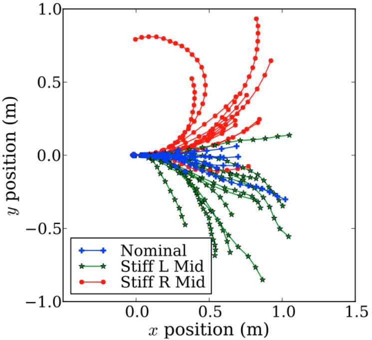

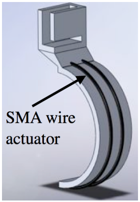

design

minimal use of actuators

Hoover et al. 2010

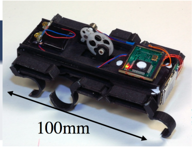

identification

control

asymmetric leg stiffness change

Proctor & Holmes 2008

Hoover, Burden, Fu, Sastry, Fearing BIOROB 2010

Robust Stability

physical system

animal, robot

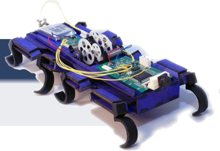

identification ↓

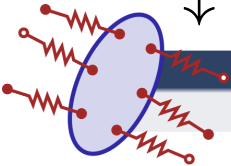

detailed model

10–100 DOF

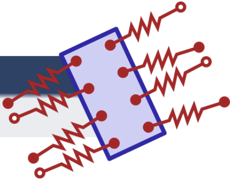

reduction ↓

↑ robustness

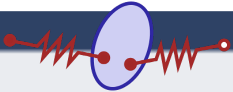

reduced-order model

< 10 DOF

Near–simultaneous hybrid transitions

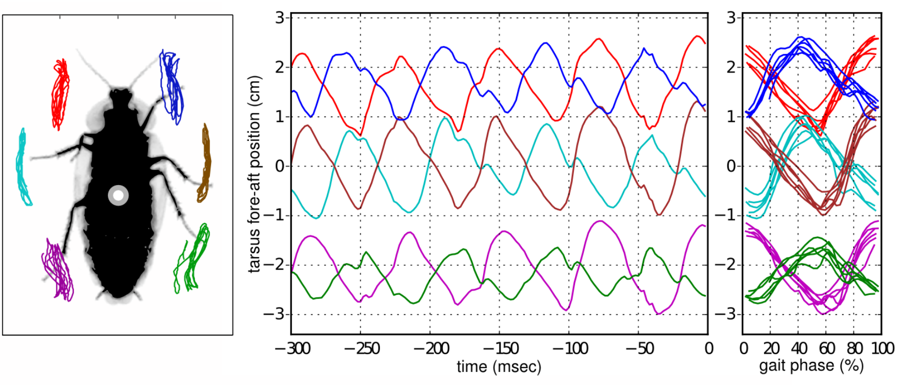

Near–simultaneous limb touchdown typical for animal gaits

Alexander IJRR 1984; Golubitsky *et al.* Nature 1999; Holmes *et al.* SIAM 2006

Near–simultaneous hybrid transitions

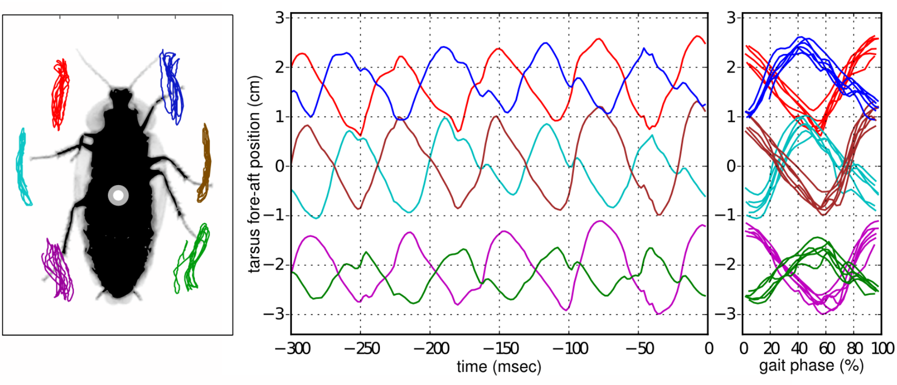

Near–simultaneous limb touchdown typical for animal gaits

Alexander IJRR 1984; Golubitsky *et al.* Nature 1999; Holmes *et al.* SIAM 2006

(Consequently) also typical for polyped robot gaits

Saranli *et al.* IJRR 2001; Kim *et al.* IJRR 2006; Hoover *et al.* IROS 2008

Pathologies in models of rigid simultaneous impact

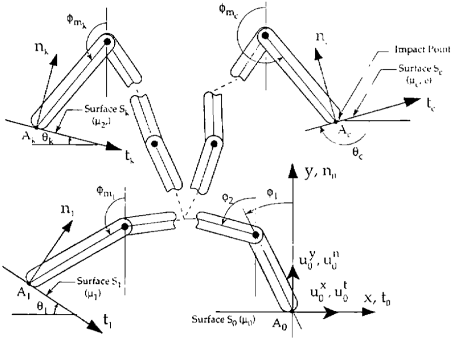

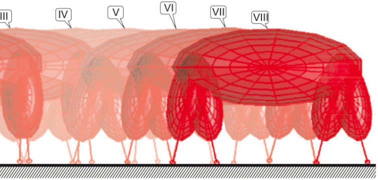

Pathologies in models of rigid simultaneous impact

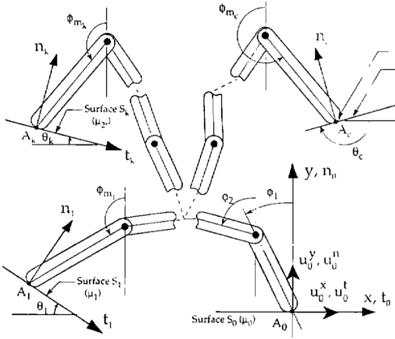

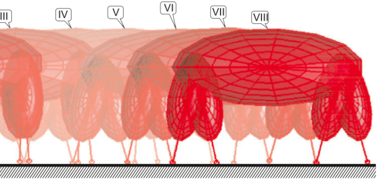

Depending on impact model, kinematic trees admit 5 (!) distinct outcomes

Hürmüzlü and Marghitu IJRR 1994

Hürmüzlü and Marghitu JAM 1995

Pathologies in models of rigid simultaneous impact

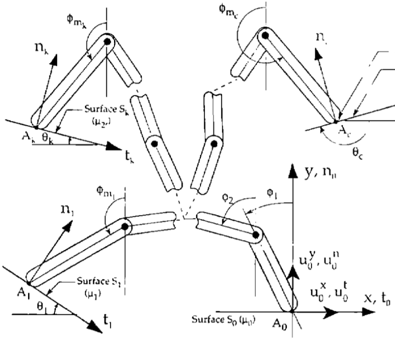

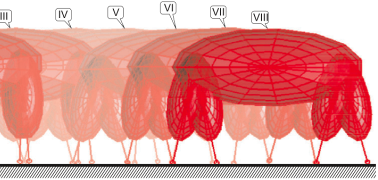

Depending on impact model, kinematic trees admit 5 (!) distinct outcomes

Hürmüzlü and Marghitu IJRR 1994

Hürmüzlü and Marghitu JAM 1995

Quadruped model possesses three distinct near–simultaneous trot gaits

Remy *et al.* IJRR 2010

Pathologies in models of rigid simultaneous impact

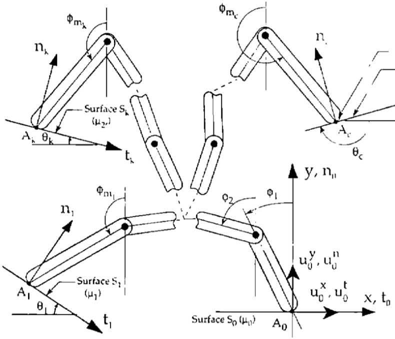

Depending on impact model, kinematic trees admit 5 (!) distinct outcomes

Hürmüzlü and Marghitu IJRR 1994

Hürmüzlü and Marghitu JAM 1995

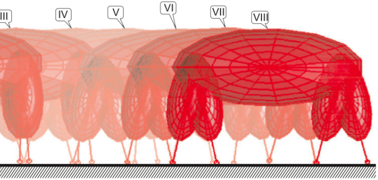

Quadruped model possesses three distinct near–simultaneous trot gaits

Remy *et al.* IJRR 2010

Need impact model that resolves inconsistencies and ambiguities

Rapid limb deceleration

U. Minnesota Equine Center

www.naturhov.dk

Rapid limb deceleration

U. Minnesota Equine Center

www.naturhov.dk

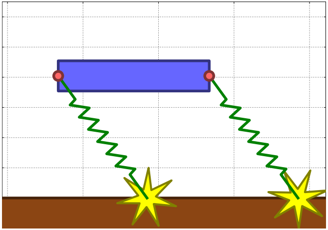

Rapid limb deceleration $\implies$ additive impulse on body

U. Minnesota Equine Center

www.naturhov.dk

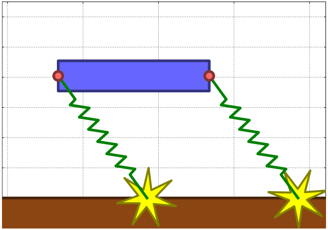

$\implies$

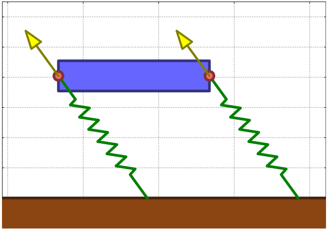

Example (reduced–order model for trot)

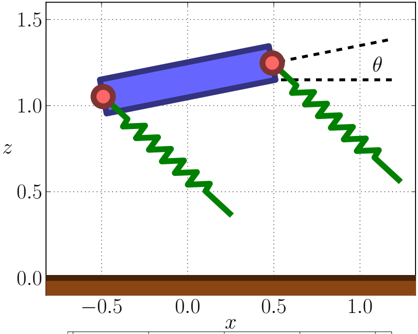

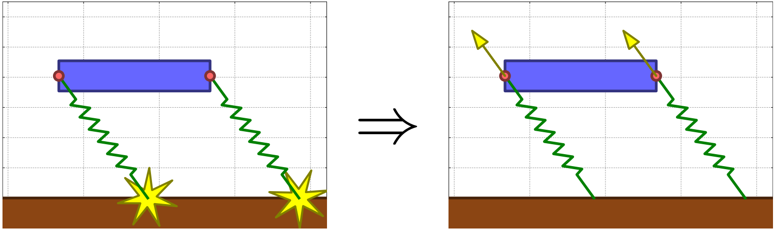

Burden, Gonzalez, Vasudevan, Bajcsy, & Sastry 2013 (arXiv:1302.4402)

Geometry of near–simultaneous limb touchdown

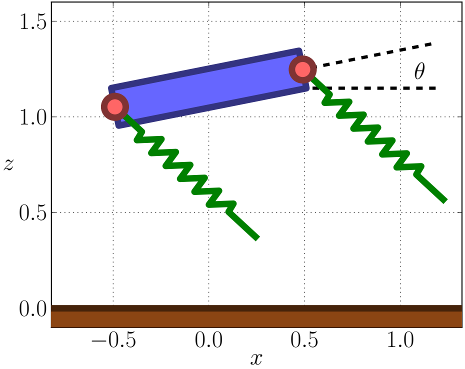

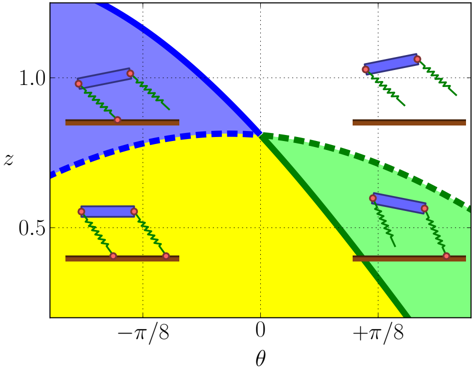

Geometry of near–simultaneous limb touchdown

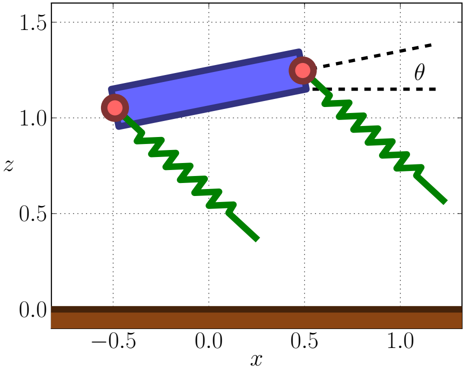

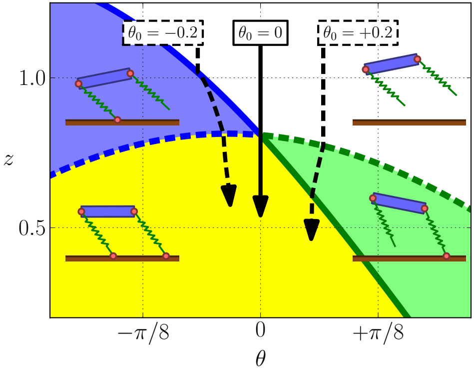

Geometry of near–simultaneous limb touchdown

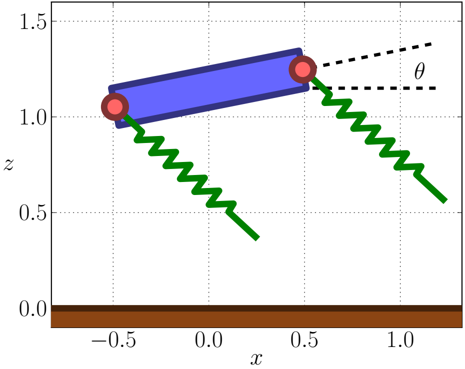

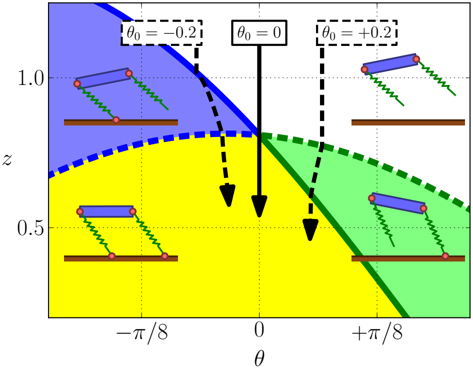

Stabilization mechanism for kinematics

Near–simultaneous impacts stabilize rotation.

Geometry of near–simultaneous limb touchdown

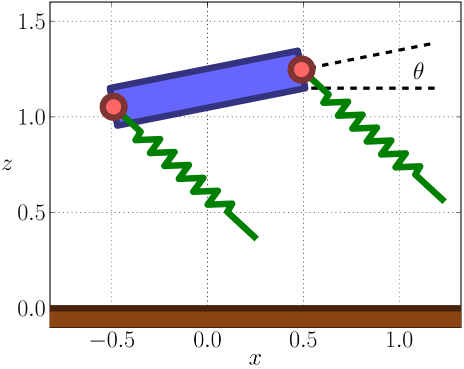

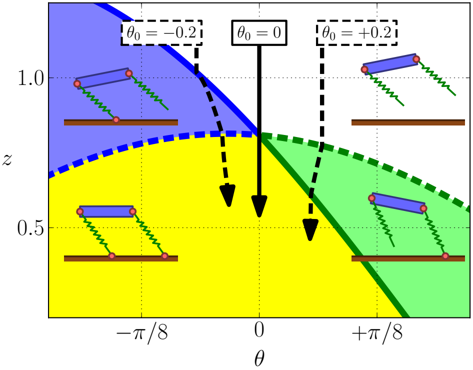

Stabilization mechanism for kinematics

Near–simultaneous impacts stabilize rotation.

Extension to dynamics

Discontinuous forces stabilize velocity.

Robust stability from non–smooth Poincaré map

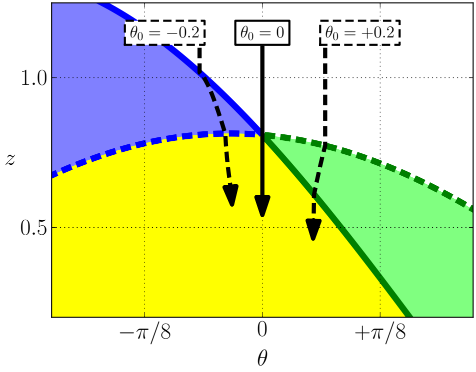

Robust stability from non–smooth Poincaré map

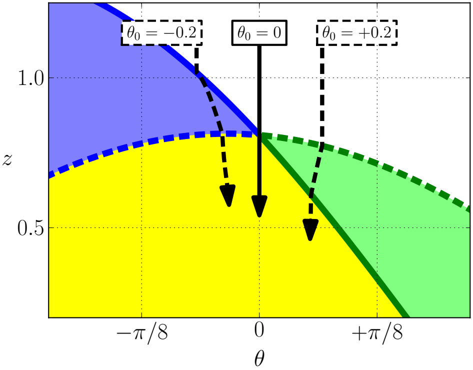

Near–simultaneous impact yields non–smooth Poincaré map

Recall: (isolated transitions $\Rightarrow$ smooth); (rigid impact $\Rightarrow$ discontinuous).

Robust stability from non–smooth Poincaré map

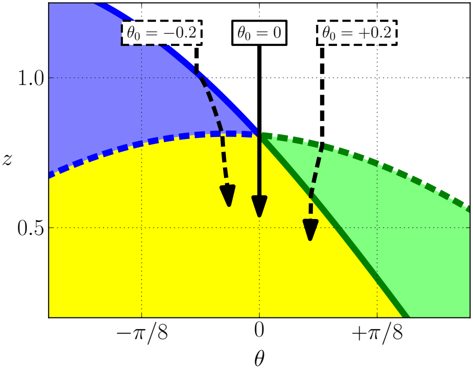

Near–simultaneous impact yields non–smooth Poincaré map

Recall: (isolated transitions $\Rightarrow$ smooth); (rigid impact $\Rightarrow$ discontinuous).

Robustness to impact uncertainty

Poincaré map can be stable for range of impulses.

Abstraction and generalization to higher dimensions

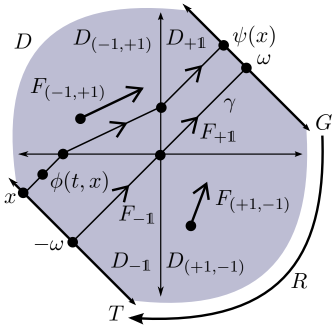

- State space $D \subset \mathbb{R}^n$
- Orthant indices $B_n = \{-1,+1\}^n$ ($|B_n| = 2^n$)
- Orthant defined for each $b \in D_b$:
  $D_b = \left\{x \in D : b^j = \operatorname{sign}\left(x^j\right)\right\}$
- Piecewise–constant vector field:
  $x \in D_b \implies \dot{x} = F_b$

Abstraction and generalization to higher dimensions

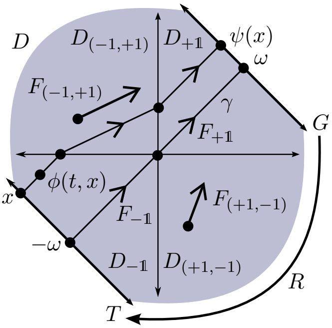

- State space $D \subset \mathbb{R}^n$
- Orthant indices $B_n = \{-1,+1\}^n$ ($|B_n| = 2^n$)
- Orthant defined for each $b \in D_b$:
  $D_b = \left\{x \in D : b^j = \operatorname{sign}\left(x^j\right)\right\}$
- Piecewise–constant vector field:
  $x \in D_b \implies \dot{x} = F_b$

- Input, output surfaces T, G
- Orthant sequences S_n ($|S_n| = n!$)
- Defining functions $\{\psi_\sigma : T \to G\}_{\sigma \in S_n}$ for

input / output map $\psi : T \to G$

Abstraction and generalization to higher dimensions

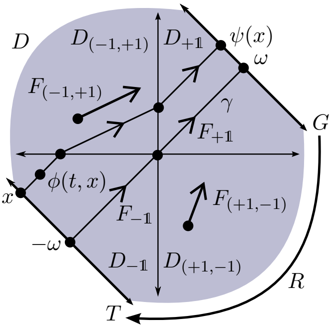

- State space $D \subset \mathbb{R}^n$
- Orthant indices $B_n = \{-1,+1\}^n$ ($|B_n| = 2^n$)
- Orthant defined for each $b \in D_b$:
  $D_b = \left\{x \in D : b^j = \operatorname{sign}\left(x^j\right)\right\}$
- Piecewise–constant vector field:
  $x \in D_b \implies \dot{x} = F_b$

- Input, output surfaces T, G
- Orthant sequences S_n ($|S_n| = n!$)
- Defining functions $\{\psi_\sigma : T \to G\}_{\sigma \in S_n}$ for input / output map $\psi : T \to G$

Theorem (Burden, Revzen, Sastry, Koditschek (*in preparation*))

$\psi : T \to G$ is continuous and piecewise–smooth; if $\psi_\sigma : T \to G$ is a contraction for all $\sigma \in S_n$, then $\psi : T \to G$ is a contraction as well.

Abstraction and generalization to higher dimensions

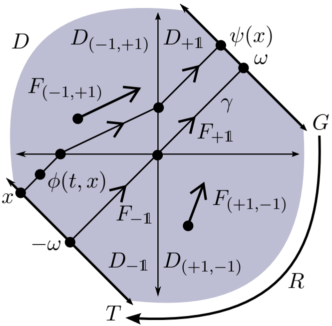

- State space $D \subset \mathbb{R}^n$
- Orthant indices $B_n = \{-1,+1\}^n$ ($|B_n| = 2^n$)
- Orthant defined for each $b \in D_b$:
  $D_b = \left\{x \in D : b^j = \operatorname{sign}\left(x^j\right)\right\}$
- Piecewise–constant vector field:
  $x \in D_b \implies \dot{x} = F_b$

- Input, output surfaces T, G
- Orthant sequences S_n ($|S_n| = n!$)
- Defining functions $\{\psi_\sigma : T \to G\}_{\sigma \in S_n}$ for input / output map $\psi : T \to G$

Theorem (Burden, Revzen, Sastry, Koditschek (*in preparation*))

$\psi : T \to G$ is continuous and piecewise–smooth; if $\psi_\sigma : T \to G$ is a contraction for all $\sigma \in S_n$, then $\psi : T \to G$ is a contraction as well.

Corollary (robustness to perturbations)

If $F_b : D_b \to TD_b$ is smooth, then contraction holds locally near $-\omega \in T$.

Gait Synthesis

physical system

animal, robot

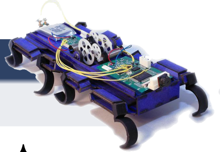

identification

synthesis

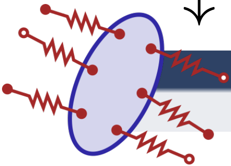

detailed model

10–100 DOF

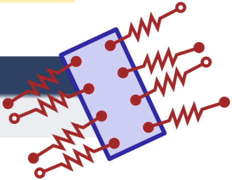

reduction

robustness

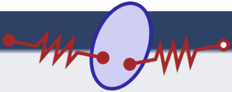

reduced-order model

< 10 DOF

Gaits designed via kinematic or virtual constraints

RHex robot (KodLab, `http://kodlab.seas.upenn.edu`)

DynaROACH robot (Olin Robotics Lab, `http://orb.olin.edu`)

Robust limb coordination for rough terrain

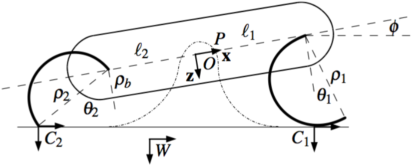

Johnson & Koditschek IEEE 2013

Robust limb coordination for rough terrain

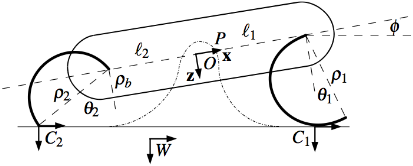

Johnson & Koditschek IEEE 2013

Smooth leg coordination

$T^2 = S^1 \times S^1$

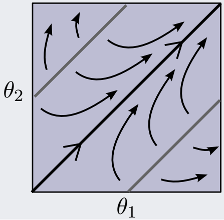

Robust limb coordination for rough terrain

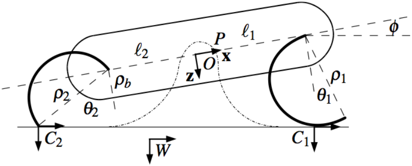

Johnson & Koditschek IEEE 2013

Smooth leg coordination

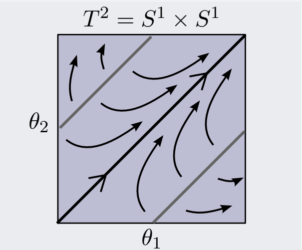

Hybrid leg coordination

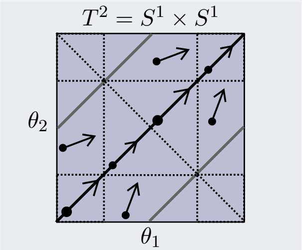

Revzen, Burden, Sastry, Koditschek DW 2013

Optimal maneuver synthesis

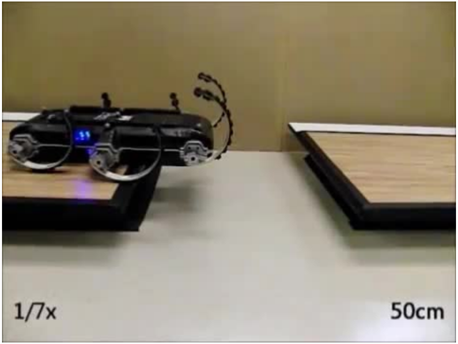

X-RHex Lite (http://kodlab.seas.upenn.edu)

Optimal maneuver synthesis

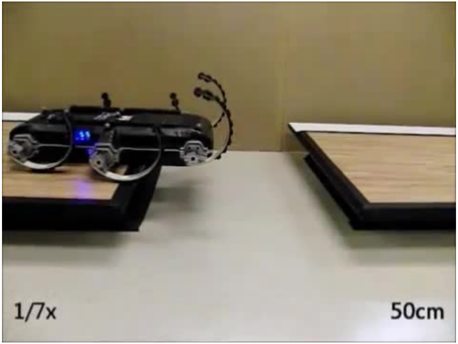

X-RHex Lite (`http://kodlab.seas.upenn.edu`)

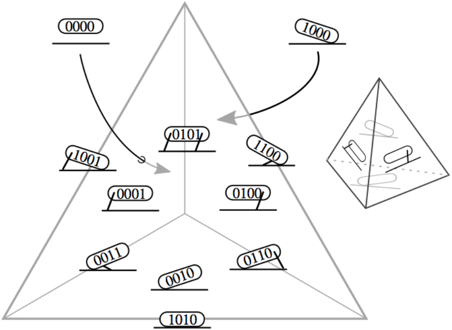

Johnson & Koditschek ICRA 2013

Optimal maneuver synthesis

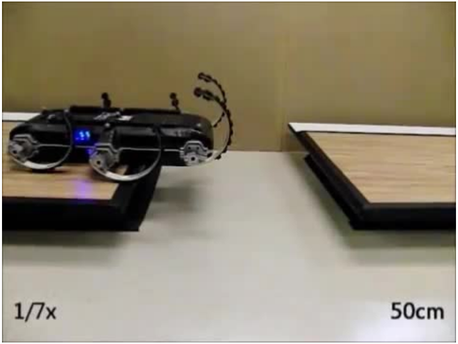

X-RHex Lite (`http://kodlab.seas.upenn.edu`)

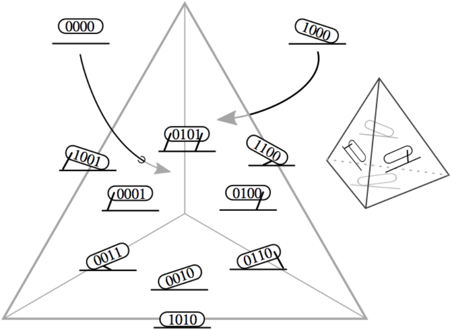

Johnson & Koditschek ICRA 2013

Reformulate combinatorial problem

Control yields footfall sequence; can search over continuous inputs.

Optimal maneuver synthesis

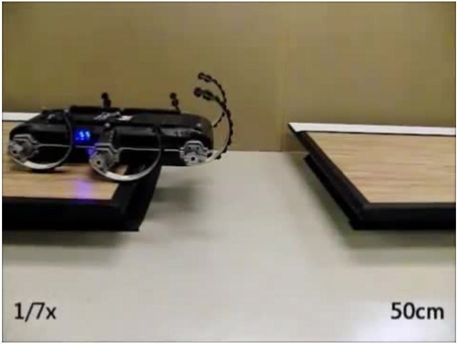

X-RHex Lite (`http://kodlab.seas.upenn.edu`)

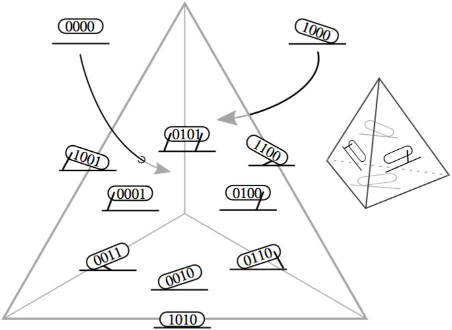

Johnson & Koditschek ICRA 2013

Reformulate combinatorial problem

Control yields footfall sequence; can search over continuous inputs.

Dynamics are continuous and piecewise–smooth

Can compute first–order variation, apply nonlinear programming.

Models enable translation across scale and morphology

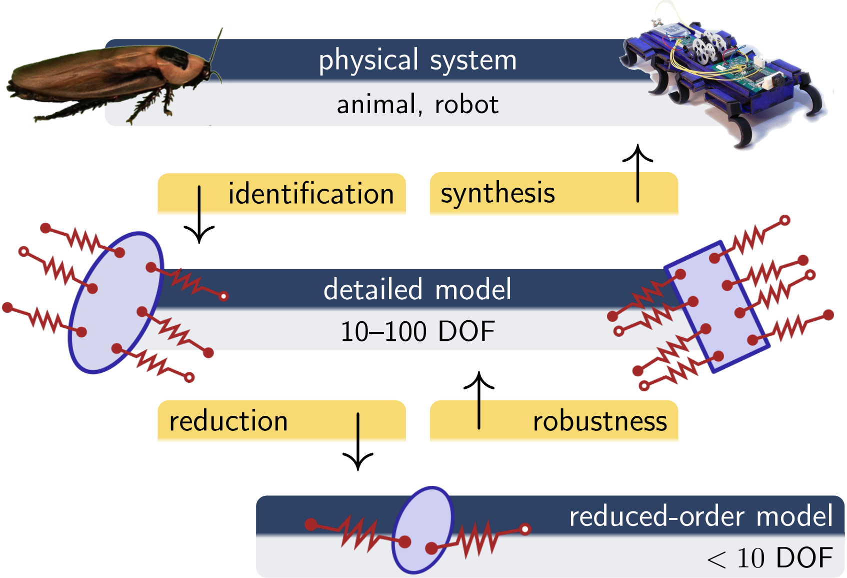

Models enable translation across scale and morphology

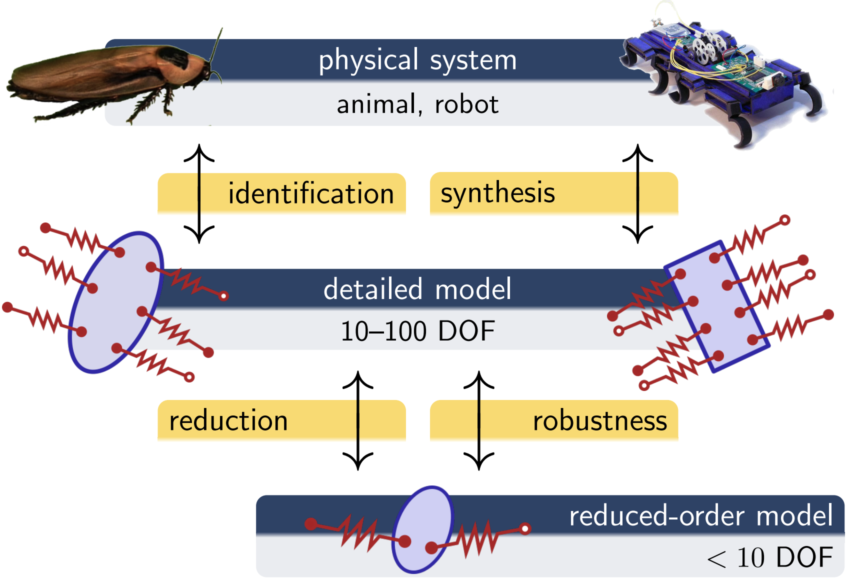

Discussion & Questions — Thanks for your time!

Reduction

– Reduced–order model emerges from intermittent contact.
– Enables scalable algorithm for parameter identification.

Robustness

– Robust stability arises from simultaneous impact.
– Enables synthesis of robust gaits and optimal maneuvers.

Collaborators

– Shankar Sastry (UCB)
– Robert Full (UCB)
– Dan Koditschek (UPenn)
– Shai Revzen (UMich)
– Aaron Hoover (Olin)
– Henrik Ohlsson (Linköping)

Funding

– NSF Fellowship
– ARL MAST CTA